Infrared reflectivity of La_2CuO_4: Anharmonic shell-model analysis

S. Koval and R. Migoni
Instituto de Física Rosario, Universidad Nacional de Rosario, Bvd. 27 de Febrero 210 Bis, 2000 Rosario, República Argentina
(Received 8 September 1994)

The infrared reflectivity (IR) of La_2CuO_4 is calculated by means of an anharmonic shell-model (SM) theory developed recently. The phonon frequencies and eigenvectors are taken from a SM fit of the experimental data in the principal symmetry directions. The phonon linewidths Γ are obtained first from the anharmonic terms of the potentials determined by fitting the phonon frequencies. The corresponding IR spectra show fairly good agreement with measurements, but this is remarkably improved by suitably varying the anharmonic terms. The frequency dependence of Γ explains certain shapes of the reflectivity bands, which led to erroneous assignments of phonons in a previous analysis of the spectra with *ad hoc* fitted Γ. The measurements show a low-frequency shoulder of the IR band corresponding to the stretching mode in the Cu-O_2 plane ($\simeq 672$ cm^{-1}). We conclude that this feature cannot be interpreted as a peculiar shape of the band due to the frequency dependence of Γ, and should be ascribed to an additional IR-active, possibly polaronic excitation.

I. INTRODUCTION

Since the discovery of the high-temperature superconductors (HTS) many efforts have been made to understand their physical properties as well as the pairing mechanism which leads to superconducting states with high critical temperatures.[1] There is a justified consensus that in the high-T_c cuprates the strong electron correlations in the Cu-O planes are most relevant to the physical properties, including the pairing mechanism.[2] However, the contribution of the electron-phonon interaction is not fully clarified and there are several effects which apparently require this interaction to be understood.[3] In order to assess quantitatively the importance of phonons and their interactions with electrons it is necessary to perform detailed calculations with realistic models.

From the lattice-dynamical point of view, the cuprate superconductors behave in general as ionic compounds in spite of the covalent character of the basal plane bonds.[2] For La_2CuO_4, neutron diffraction measurements of phonons in all the principal symmetry directions[4] were fitted accurately with a shell model (SM).[5] However, the size and quality of the single crystals, strong anharmonicity, and the interpretation of measurements in the orthorhombic phase were serious complications which led to an erroneous analysis of the data. Further measurements and a very careful analysis allowed confident determination of phonon frequencies, which showed important differences with the previous ones. This last set of data was well fitted again with a shell model.[6]

The infrared reflectivity (IR) spectra of La_2CuO_4 have been measured with the incident radiation polarized parallel[7,8] (xy spectrum) and perpendicular[8] (z spectrum) to the Cu-O_2 planes. The xy spectrum is expected to show four bands of maximum reflectivity corresponding to the four IR-active E_{2u} modes with xy polarization. However, only three of these bands are observed, which led to several spectulations. One of these was that the missing band is overlapped either with the one centered at $\simeq 180$ cm^{-1} or with the peak at $\simeq 360$ cm^{-1}. Another interpretation was that this phonon is located in the low-frequency range and is out of the measuring range. In Ref. 7 it was concluded that the missing band most probably corresponds to an apex bending mode with small oscillator strength and overlaps with the dominant phonon at $\simeq 140$ cm^{-1}.

The lattice dielectric response of La_2CuO_4 was recently calculated with a harmonic SM,[9] but the model parameters were fitted only to the Brillouin zone center modes and *ad hoc* values of the phonon linewidths were used to fit the experimental reflectivity data. The last point seems to be crucial in explaining both why a fourth band is missing in the xy spectrum, and several details in the shape of the reflectivity bands.[9]

In the present paper we calculate the far-infrared optical reflectivity using a SM with two-body central potentials for the short-range interactions, which gives a good description of the measured phonon dispersion in all the principal symmetry directions of tetragonal La_2CuO_4.[6] The TO phonon linewidths $\Gamma_j(\omega)$ are calculated by using an anharmonic SM perturbation theory,[10] which we previously applied successfully to obtain the optical zone-center phonon linewidth and line shift in silicon.[11] The anharmonic terms in the expansion of the model potentials are tested by using them in the expression for $\Gamma_j(\omega)$. However, the IR spectra are better adjusted by suitably choosing the anharmonic force constants.

II. THE MODEL AND RESULTS

We use the SM cited above[6] to calculate the frequencies and eigenvectors of the infrared-active modes. The linewidths of these phonons are calculated using the perturbative formalism for an anharmonic SM described in Ref. 11. We considered the third-order force constants arising from the derivatives up to third order of both the short-range and Coulomb potentials.

The total crystal potential developed up to third order in the core and shell displacements is then written as follows

$$\Phi(\mathbf{u},\mathbf{v})=\sum_{l\kappa\alpha}\sum_{l'\kappa'\beta}[\tfrac{1}{2}u_\alpha(l\kappa)u_\beta(l'\kappa')+u_\alpha(l\kappa)v_\beta(l'\kappa')+\tfrac{1}{2}v_\alpha(l\kappa)v_\beta(l'\kappa')]\Phi^S_{\alpha\beta}(l\kappa,l'\kappa')$$
$$+\sum_{l\kappa\alpha}{}'\sum_{l'\kappa'\beta}{}'\{\tfrac{1}{2}X_\kappa X_{\kappa'}[u_\alpha(l\kappa)u_\beta(l'\kappa')-u_\alpha(l\kappa)u_\beta(l\kappa)]+\tfrac{1}{2}Y_\kappa Y_{\kappa'}[v_\alpha(l\kappa)v_\beta(l'\kappa')-v_\alpha(l\kappa)v_\beta(l\kappa)]$$
$$+X_\kappa Y_{\kappa'}[u_\alpha(l\kappa)v_\beta(l'\kappa')-\tfrac{1}{2}u_\alpha(l\kappa)u_\beta(l\kappa)-\tfrac{1}{2}v_\alpha(l'\kappa')v_\beta(l'\kappa')]\}\Phi^C_{\alpha\beta}(l\kappa,l'\kappa')+\Phi^S_3(\mathbf{v})+\Phi^C_3(\mathbf{u},\mathbf{v}) , \quad (2.1)$$

where $\Phi^S_3(\mathbf{v})$ contains the cubic shell-shell interactions for the nearest-neighbor two-body central potentials and $\Phi^C_3(\mathbf{u},\mathbf{v})$ represents the third-order terms of the Coulomb potential, which have the following expression:

$$\Phi^C_3(\mathbf{u},\mathbf{v})=\sum_{l\kappa}{}'\sum_{l'\kappa'}{}'\sum_{\alpha\beta\gamma}[X_\kappa(X_{\kappa'}+Y_{\kappa'})u_\alpha(l\kappa)u_\beta(l\kappa)u_\gamma(l\kappa)+X_\kappa X_{\kappa'}u_\alpha(l\kappa)u_\beta(l'\kappa')u_\gamma(l'\kappa')$$
$$+Y_\kappa(X_{\kappa'}+Y_{\kappa'})v_\alpha(l\kappa)v_\beta(l\kappa)v_\gamma(l\kappa)+Y_\kappa Y_{\kappa'}v_\alpha(l\kappa)v_\beta(l'\kappa')v_\gamma(l'\kappa')$$
$$+X_\kappa Y_{\kappa'}u_\alpha(l\kappa)v_\beta(l'\kappa')v_\gamma(l'\kappa')+Y_\kappa X_{\kappa'}v_\alpha(l\kappa)u_\beta(l'\kappa')u_\gamma(l'\kappa')]\Phi^C_{\alpha\beta\gamma}(l_\kappa,l'\kappa') . \quad (2.2)$$

In Eqs. (2.1) and (2.2), $u_\alpha(l\kappa)$ and $v_\alpha(l\kappa)$ are the core and shell absolute displacements. $\Phi^S_{\alpha\beta}(l\kappa,l'\kappa')$ is the harmonic shell-shell interaction and $\Phi^C_{\alpha\beta}(l\kappa,l'\kappa')$ and $\Phi^C_{\alpha\beta\gamma}(l\kappa,l'\kappa')$ are the harmonic and cubic Coulomb force constants. The last ones are considered only between nearest neighbors. X_κ and Y_κ are the core and shell charges for the κ ion in the unit cell. The primes mean that the summation runs over $(l'\kappa')\neq(l\kappa)$. The short-range interactions couple only nearest-neighbor shells with Born-Mayer potential (a Van der Waals term is added for the O-O interaction). The model parameters are given in Ref. 6.

Each short-range interaction in $\Phi^S_3(\mathbf{v})$, as well as each Coulomb interaction in $\Phi^C_3(\mathbf{u},\mathbf{v})$, contributes with a diagram of type (b) in Ref. 11 to the linewidth, which can then be written as

$$\Gamma_j(\omega)=\frac{\pi\hbar}{16N}\sum_{\mathbf{q}j_1j_2}\left|\sum_t X^{(3)}_t(\mathbf{0}j,\mathbf{q}j_1,-\mathbf{q}j_2)\right|^2$$
$$\times D[\omega,\omega^0(\mathbf{q}j_1),\omega^0(\mathbf{q}j_2)] , \quad (2.3)$$

where all the quantities are explained in Ref. 11. The subscript t distinguishes different interactions. The five of short-range type are listed in Table I. The corresponding $X^{(3)}_t$ are all of the same form, Eqs. (A3), (A6), and (A7) of Ref. 11. The Coulomb interaction $\Phi^C_3(\mathbf{u},\mathbf{v})$ includes terms with core as well as shell displacements. Whenever a core displacement appears, the corresponding eigenvector $\mathbf{e}(\mathbf{q}j)$ must replace the shell eigenvector $C(\mathbf{q})\mathbf{e}(\mathbf{q}j)$ in (A7) of Ref. 11.

The reflectivity is calculated from the dielectric function

$$\epsilon_{\alpha\beta}(\omega)=\epsilon_{\alpha\beta}(\infty)+\sum_j\frac{S_{\alpha\beta}(j)}{\omega^{j^2}-\omega^2-i\omega\Gamma_j(\omega)} , \quad (2.4)$$

where, for the shell model,[12]

$$S_{\alpha\beta}(j)=\frac{4\pi e^2}{\Omega}p_\alpha(j)p^*_\beta(j) \quad (2.5)$$

with

$$p_\alpha(j)=\sum_k\left[Z_\kappa\frac{e^\alpha_\kappa(j)}{\sqrt{m_\kappa}}+Y_\kappa\sum_{\kappa'\beta}F^{\alpha\beta}_{\kappa\kappa'}\frac{e^\alpha_\kappa(j)}{\sqrt{m_\kappa}}\right] . \quad (2.6)$$

The expressions for $\epsilon_{\alpha\beta}(\infty)$ and $F^{\alpha\beta}_{\kappa\kappa'}$ are given in Ref. 12.

In Figs. 1 and 2 we plot the xy and z spectra, respectively. The solid circles represent the experimental data[7,8] and the dashed lines are the calculated spectra with the linewidths of the TO phonons computed from

TABLE I. Third derivatives of the short-range potential for the different nearest-neighbor atom pairs (the notation is that of Ref. 5). The values in the upper row are derived from the SM potentials (Ref. 6) and the ones in the lower row are fitted to the IR data. The units are eV/Å^3.

Cu-O_{xy}	Cu-O_z	La_z-O_{xy}	La_z-O_z	O_x-O_y
−84.85	−7.42	−17.39	−39.07	−2.13
61.90	−18.14	−8.01	48.42	−15.43

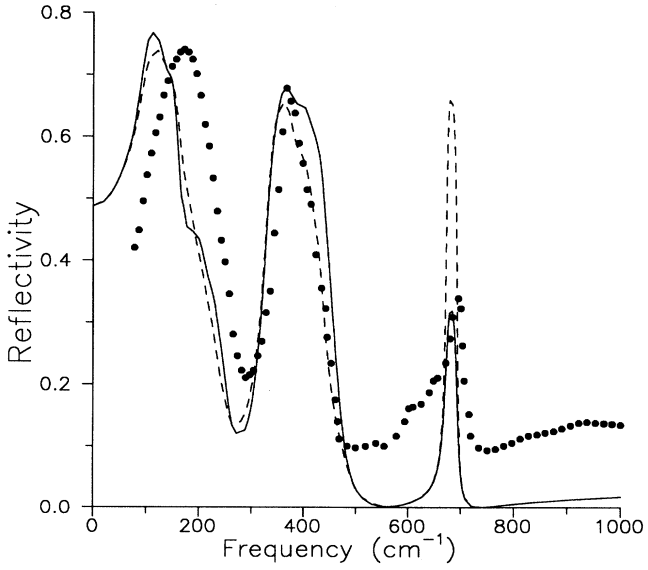

FIG. 1. Reflectivity for the incident electric field along the xy plane vs. frequency. The solid line corresponds to fitted anharmonic parameters and the dashed line is obtained with anharmonic parameters derived from the SM potentials of Ref. 6. The solid circles are the experimental data of Ref. 7.

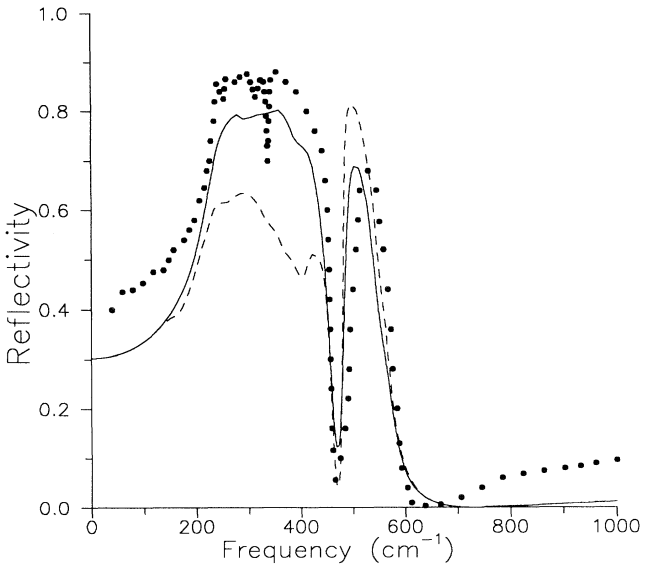

FIG. 2. The analog of Fig. 1 for the exciting field along z. The experimental data are from Ref. 8.

the SM potential parameters as previously explained.

The values of the third derivatives of the potentials are given in the upper row of Table I. The overall agreement with the experimental spectra is much better than in the previous SM calculation with *ad hoc* values of the damping parameters.[9] All reflectivity bands are fairly well reproduced. The calculated high-frequency dielectric constants $\epsilon_{xx}(\infty)$ and $\epsilon_{yy}(\infty)$ turn out to be low compared with the experimental values, as can be seen in Tables II and III. This reveals that the electronic polarizability is not fully described in the present SM and this is responsible for the low value of the calculated reflectivity compared with the experimental data at high frequencies, as it is seen in Figs. 1 and 2. According to our calculation, the xy spectrum shows only three reflectivity bands because the oscillator strength $S_{xx}(2)$ is two orders of magnitude smaller than that of the other three E_{2u} modes (see Table II). This fact is also revealed by the dielectric function $\epsilon_{xx}(\omega)$ in Fig. 3. $\mathrm{Re}[\epsilon_{xx}(\omega)]$ exhibits a very small peak at $\simeq 168$ cm^{-1}, and also a weak structure appears at this frequency in $\mathrm{Im}[\epsilon_{xx}(\omega)]$. The mode $j=2$ involves bending of the Cu–apex O bonds produced by the vibration of the apex oxygen sublattice parallel to and against almost rigid Cu-O_2 planes. As argued in Ref. 7, the weak oscillator strength of this mode is related to its resemblance to the silent mode in the ideal perovskite structure. In Fig. 1, the shift of the first peak to lower frequencies in the calculation is equal to the difference between the SM frequency of the lowest E_{2u} mode and the neutron diffraction data (see Table II). The little shoulder appearing in the calculation on the right side of the second peak, at $\simeq 400$ cm^{-1}, is due to the frequency dependence of $\Gamma_3(\omega)$. This feature appears also in the experiment, and was wrongly fitted with a fictitious phonon at 400 cm^{-1} by the procedure based on the oscillator model.[7]

In the z spectrum (Fig. 2), the broadband between $\simeq 230$ and $\simeq 450$ cm^{-1} arises from the large LO-TO split-

TABLE II. Frequencies of the transverse (ω_j) and longitudinal [ω_j(LO)] modes, oscillator strengths $S_{xx}(j)$, and linewidths at the mode frequency $\Gamma_j(\omega_j)$ of the xy-polarized E_{2u} modes. The values of $\Gamma_j(\omega_j)$ corresponds to the fitted anharmonic parameters in the second row of Table I. The dominant contributions to $\Gamma_j(\omega_j)$ are given in the last column, where C denotes the Coulomb interaction. ω and Γ are given in cm^{-1} and S in cm^{-2}. The calculated and experimental values of the high-frequency dielectric constant $\epsilon_{xx}(\infty)$ are also given.

	This work	IR (Ref. 7)	IR (Ref. 8)	Neutron diffraction (Ref. 6)	Dominant anharmonicities
ω_1	98	145	132	126	La_z-O_z
ω_1(LO)	168			171	
$10^{-3}S_{xx}(1)$	856	488	624		
$\Gamma_1(\omega_1)$	66	45	52		
ω_2	168	(400)?		171	C, La_z-O_z
ω_2 (LO)	260			279	
$10^{-3}S_{xx}(2)$	4.8	(48)?			
$\Gamma_2(\omega_2)$	19	(60)?			
ω_3	330	360	358	350	C, La_z-O_{xy}
ω_3 (LO)	461			459	
$10^{-3}S_{xx}(3)$	328	233	305		
$\Gamma_3(\omega_3)$	54	20	28		
ω_4	673	695	667	675	O_x-O_y, C
ω_4 (LO)	692			679	
$10^{-3}S_{xx}(4)$	114	174	168		
$\Gamma_4(\omega_4)$	25	27	16		
$\epsilon_{xx}(\infty)$	1.092	6.0	5.5		

TABLE III. The same quantities as in Table II for the z-polarized A_{2u} modes.

	This work	IR (Ref. 7)	Neutron diffraction (Ref. 6)	Dominant anharmonicities
ω_1	134	(342)?	150	C, Cu-O_z
ω_1(LO)	134		150	
$10^{-3}S_{zz}(1)$	0.1	8.5		
$\Gamma_1(\omega_1)$	20	4		
ω_2	229	242	228	C, La_z-O_z, Cu-O_z
ω_2(LO)	460		468	
$10^{-3}S_{zz}(2)$	1597	1000		
$\Gamma_2(\omega_2)$	83	30		
ω_3	480	501	498	C, Cu-O_z
ω_3(LO)	566		570	
$10^{-3}S_{zz}(3)$	64	92		
$\Gamma_3(\omega_3)$	29	20		
$\epsilon_{zz}(\infty)$	1.089	4.75		

ting of the A_{2u} mode 2 in Table III. The sharp depression of this band at $\simeq 330$ cm^{-1} led wrongly to the assignation of a phonon by the oscillator fit of Ref. 8. This depression should be ascribed actually to a peak in the linewidth $\Gamma_2(\omega)$ as a function of frequency. This is plotted as a dashed line in Fig. 4. We observe a peak at $\simeq 400$ cm^{-1}, and a depression of the calculated band (dashed line of Fig. 2) is seen around the same frequency. There are three z-polarized A_{2u} modes which are allowed to contribute to the z spectrum. However, only two bands are observed, and this is also explained by our results. In fact, a look at Table III reveals that the oscillator strength of mode 1 is so weak compared with the other two A_{2u} modes that it does not give any contribution to the reflectivity. It also does not show up in the dielectric function $\epsilon_{zz}(\omega)$, plotted in Fig. 5. This mode is roughly a vibration along the z axis of apex oxygen and La ions against the Cu-O_2 planes. The third peak of the xy spectrum comes out too high in the calculation with the SM potentials, while the intensity of the broadband in the z spectrum turns out to be rather weak. We ascribed these failures of the model to the phonon linewidths arising from the third derivatives of the short-range potentials. Therefore we determine these five values such as to reproduce the intensities of the five bands in the xy and z spectra. The resulting parameters are given in the second row of Table I and the corresponding spectra are plotted with solid lines in Figs. 1 and 2. We observe drastic changes in all these parameters, particularly the sign changes in the Cu-O_{xy} and La_z-O_z third derivatives.

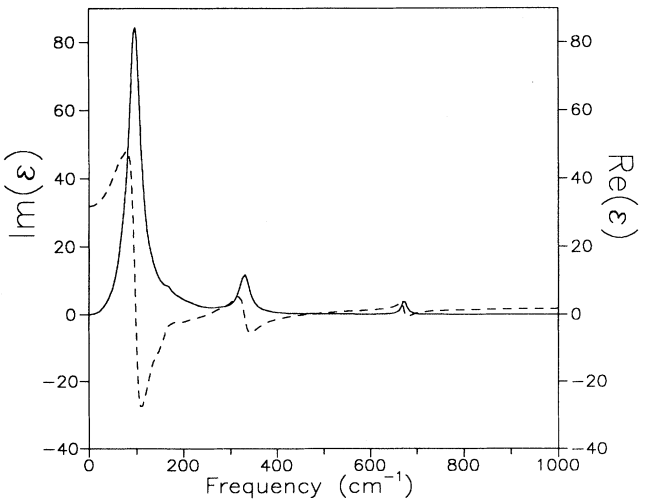

FIG. 3. Real and imaginary parts of the dielectric function $\epsilon_{xx}(\omega)$. Note the weak structures at 168 cm^{-1}.

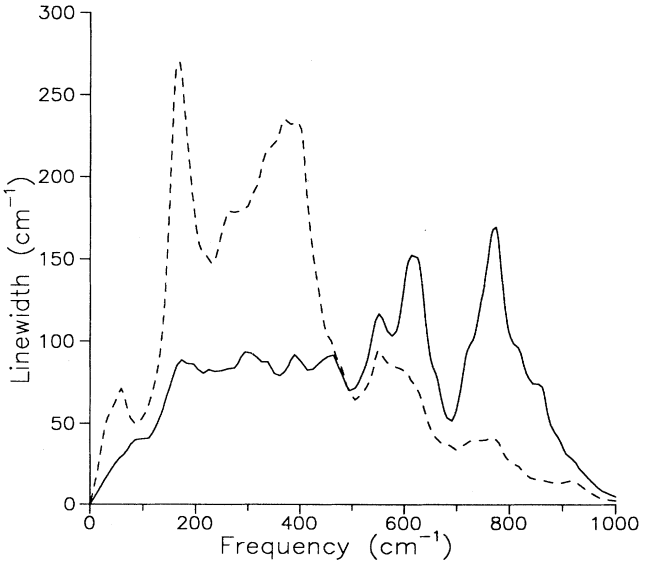

FIG. 4. Linewidth of the A_{2u} mode at 229.5 cm^{-1} as a function of frequency. The solid line corresponds to fitted anharmonic parameters and the dashed line is the result with the potential parameters derived from Ref. 6.

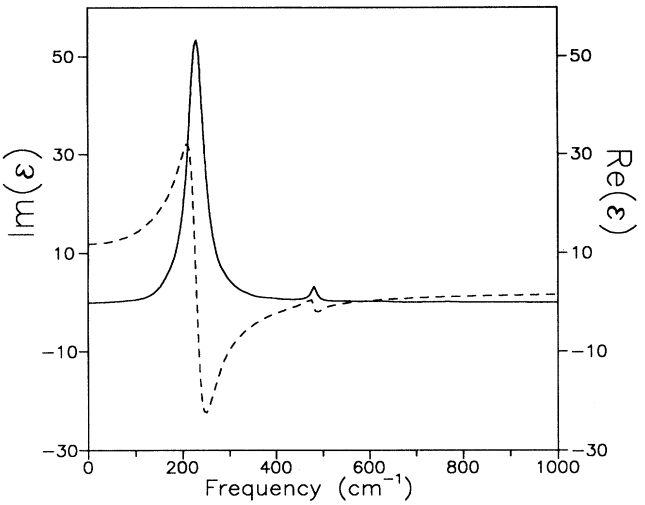

FIG. 5. The analog of Fig. 3 for the exciting field along z.

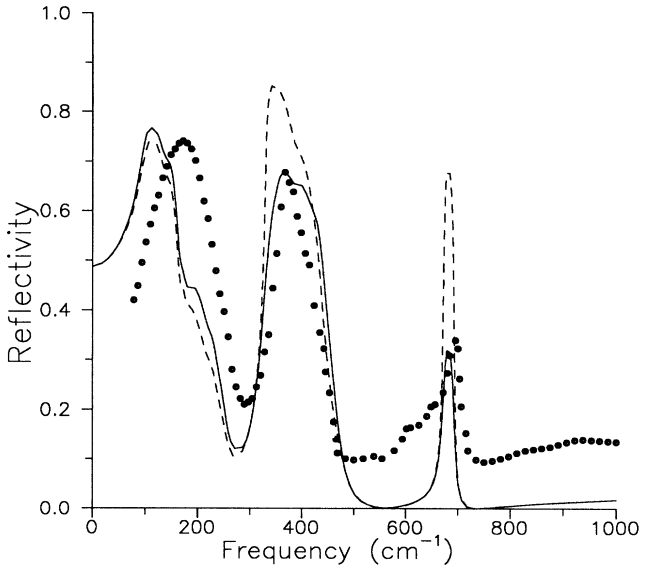

FIG. 6. The analog of Fig. 1, but the dashed line is now the IR calculated with the fitted anharmonic parameters without the contribution of the Coulomb interaction.

Now the calculation is in better agreement with experiment. However, the modified linewidth $\Gamma_2(\omega)$, plotted as a solid line in Fig. 4, does not show a well-defined peak within the frequency range of the broadband in the z spectrum. Consequently, the solid line for this spectrum does not exhibit in the broadband any significant depression analogous to experiment. The intensity of this band could not be fitted exactly due to interference with the second band.

The peak of the xy spectrum at $\simeq 680$ cm^{-1} is due to the stretching mode of the Cu-O bonds in the Cu-O_2 planes (mode 4 in Table II). The wide shoulder seen in the experimental spectrum at the low-frequency side of this peak is absent in our calculation. We note that the width of this band in the calculation corresponds to the LO-TO splitting due to the macroscopic electric field for the stretching mode. The same splitting is found in the neutron diffraction experiments.[6] Therefore the reflectivity increase below the TO frequency at 673 cm^{-1} cannot be explained as a phonon resonance in the dielectric function. For this reason, the big peak shoulder in the IR spectrum seems to have other origin than simply the phonon-phonon interaction. We also want to point out that a stretching-mode bleaching is observed in photoinduced absorption spectra and is related to possible polaron formation when carriers are photoinduced in the pure compound.[13] The same effect is also seen in La_2CuO_{4+x} with increasing oxidation.[14] We note that in the La_2CuO_4 samples where the IR was measured,[7] a low concentration of holes was not discarded. All these facts provide support for the argument that the electron-phonon interaction gives rise to an additional structure aside from this phonon in the response function. This is also concluded from cluster model calculations where the electron-phonon interaction is taken into account together with strong electron correlations at the copper site.[15]

Finally, in order to test how important is the contribution of the third-order Coulomb terms to the IR spectra, we cancel these terms and perform a calculation with only the fitted short-range parameters of the second row in Table I. the result for the xy spectrum is plotted as a dashed line in Fig. 6. We observe that the Coulomb anharmonicity makes a significant contribution to the spectrum, and the same conclusion is obtained from the z spectrum. Therefore it should not be neglected as was done in previous anharmonic calculations for ionic compounds.[16]

III. CONCLUSIONS AND DISCUSSION

We have calculated the infrared optical reflectivity spectra of La_2CuO_4 using an anharmonic SM perturbation theory to obtain frequency-dependent linewidths. A SM fitted to the phonons measured in the principal symmetry directions[6] was used to obtain the eigenfrequencies, eigenvectors, and anharmonic parameters to calculate the linewidths. These quantities enter the expressions for the dielectric function. Our results are improved with respect to those of a previous SM calculation[9] for two reasons.

(1) The former SM parameters were determined with only the zone-center phonon frequencies.[17]

(2) *Ad hoc* fixed values were used for the linewidths in Ref. 9. The last point seems to be a serious handicap for the interpretation of the detailed structure of the IR spectra. For instance, in previous oscillator-model fits certain structures have been ascribed to fictitious modes while we demonstrate here that these features are originated by the particular frequency dependence of the linewidths. The most remarkable example of this behavior is the sharp depression in the first broadband of the z spectrum.

For the exciting field along the xy plane, we obtain the first two reflectivity bands in very good agreement with the experimental data. The last peak corresponds to the stretching mode and its low-frequency shoulder is not accounted for by our calculation, leading to the conclusion

that other interactions than anharmonicity may play an important role. This interpretation is supported by the observed bleaching of the stretching mode in photoinduced carrier experiments.[13] We note that previous electron-phonon models[15] predict the mixing of this phonon with a polaronic excitation, which produces a little but well-defined peak on the low-frequency side of the infrared phonon peak. Such an effect might also explain the shoulder of the reflectivity peak for the stretching mode. Compared to the experiment, this peak is too high in the calculation with the original SM potential parameters. We achieved a reduction of this peak by drastically changing the anharmonic interactions, such that the linewidth at the phonon frequency is increased by about a factor of 3 up to the value $\simeq 25$ cm^{-1} shown in Table II.

As an alternative mechanism, a possible coupling to the polaron could cause transfer of intensity towards lower frequencies, which might render unnecessary the assumption of additional anharmonic or electron-phonon linewidth of the stretching mode to reduce the intensity of its reflectivity band.

On the other hand, we confirm that the band missing from the xy spectrum corresponds to the E_{2u} apex bending mode at $\simeq 168$ cm^{-1}, which has an oscillator strength much smaller than the other phonons, as was speculated in Ref. 7 from symmetry reasons.

The z spectrum is qualitatively reproduced by the calculation with anharmonic force constants from the SM potentials, but the intensities come closer to the experimental ones by fitting the anharmonic parameters. We find that the measured sharp depression of the first broadband at $\simeq 330$ cm^{-1} must be ascribed to a peak in the corresponding phonon linewidth as a function of frequency. The oscillator strength of an A_{2u} mode below this band is so weak that it does not produce any structure in the spectrum, which is in agreement with the measurement. Since the dipole moment of this mode nearly vanishes in a nontrivial way, this agreement in addition to an overall good reproduction of the spectra, including another almost silent E_{2u} mode, are indications that the present SM gives realistic eigenvectors for the zone-center modes.

Finally, we remark our observation that the Coulomb anharmonicity contributes significantly to the phonon linewidth and should not be neglected in calculations for ionic systems.

ACKNOWLEDGMENTS

We gratefully acknowledge Dr. L. Pintschovious and Dr. W. Reichardt for providing us experimental data and commentaries on the phonons in La_2CuO_4 as well as the parameters of the shell model they fitted to these data. We give thanks to Dr. A Dobry for helpful discussions on the coupling of the stretching mode to a polaron. We acknowledge support from the Consejo Nacional de Investigaciones Científico Técnicas.

[1]For reviews and discussion, see *High Temperature Superconductivity,* edited by J. W. Lynn (Springer, Berlin, 1990); *Theories of High Temperature Superconductivity,* edited by J. Woods Hatley (Addison-Wesley, Reading, MA, 1988).

[2]For reviews and discussion, see B. Batlogg, Phys. Today **44**(6), 44 (1991); P. W. Anderson and R. Schrieffer, Phys. Today **44**(6), 54 (1991).

[3]S. Barišič, Int. J. Mod. Phys. B **5**, 2439 (1991).

[4]L. Pintschovius in *Proceedings of the Third International Conference on Phonon Physics,* edited by S. Hunklinger, W. Ludwig, and G. Weiss (World Scientific, Singapore, 1990), p. 217; L. Pintschovius, *et al.*, in *International Seminar on High Temperature Superconductors,* edited by V. Aksenov, N. Bogolubov, and N. Plakida (World Scientific, Singapore, 1990), p. 36.

[5]S. Koval *et al.*, J. Phys. Condens. Matter. **4**, 4759 (1992).

[6]S. L. Chaplot, *et al.*, in *Physical Properties of High-Temperature Superconductors IV,* edited by D. M. Ginsberg (World Scientific, Singapore, 1994), p. 295.

[7]S. Tajima *et al.*, Phys. Rev. B **43**, 10 496 (1991).

[8]R. T. Collins *et al.*, Phys. Rev. B **39**, 2251 (1989).

[9]H. Chen and J. Callaway, Physica C **210**, 309 (1993).

[10]A. Dobry, A. Greco, and O. S. Zandron, Phys. Rev. B **43**, 1084 (1991); A. Greco, S. Koval, and R. Migoni, J. Phys. Condens. Matter **4**, 5291 (1992).

[11]S. Koval and R. Migoni, Phys. Rev. B **49**, 998 (1994).

[12]H. Chen and J. Callaway, Phys. Rev. B **45**, 2085 (1992).

[13]Y. H. Kim *et al.*, Phys. Scr. **T27**, 19 (1989); D. Mihailovič *et al.*, Phys. Rev. B **44**, 237 (1991).

[14]J. Falck *et al.*, Phys. Rev. B **48**, 4043 (1993); G. Thomas *et al.*, *ibid.* **47**, 11 369 (1993).

[15]K. Yonemitsu *et al.*, Phys. Rev. Lett. **69**, 965 (1992); A. Dobry *et al.*, *ibid.* **49**, 505 (1994).

[16]R. Heid and H. Rietschel, Phys. Rev. B **44**, 734 (1991).

[17]M. Monstoller *et al.*, Phys. Rev. B **41**, 6488 (1990).